

---

REVISTA  
**PESQUISA  
NAVAL**

---

NUMBER 28 - 2016

---



DIRECTORATE-GENERAL FOR NUCLEAR AND TECHNOLOGICAL  
DEVELOPMENT OF THE NAVY (DGDNTM)



---

REVISTA

# PESQUISA NAVAL

NUMBER 28 - 2016

---

REVISTA  
**PESQUISA  
NAVAL**

The mission of the *Revista Pesquisa Naval* is to provide a formal channel of communication and dissemination of national scientific and technical productions for the scientific community, by publishing original articles that are a result of scientific research and contribute to the advancement of knowledge in areas of interest for the Brazilian Navy. Articles published in the journal do not reflect the position or the doctrine of the Navy and are the sole responsibility of the authors.

#### SPONSORSHIP

Directorate-General for Nuclear and Technological Development of the Navy - DGDNTM

#### EDITOR-IN-CHIEF

**Admiral Bento Costa Lima Leite de Albuquerque Junior**

*Director General of Nuclear and Technological Development of the Navy*

#### ASSISTANT EDITORS

**RADM Alfredo Martins Muradas**

*Director of Naval Systems Analysis Center - CASNAV*

**RADM Marcos Lourenço de Almeida**

*Director of Admiral Paulo Moreira Marine Institute - IEAPM*

**RADM (NE) André Luis Ferreira Marques**

*Director of the Technological Center of the Navy in São Paulo*

**RADM (NE) Luiz Carlos Delgado**

*Director of Navy Research Institute - IPqM*

#### EDITORIAL BOARD

**CAPT Antônio Capistrano de Freitas Filho**

**CAPT José Fernando De Negri**

**CDR Benjamin Dante Rodrigues Duarte Lima**

**LCDR (NE) Elaine Rodino da Silva**

**2SG-RO Rogério Augusto dos Santos**

**3SG-ELEC Renato Ellyson Oliveira Cavalcante**

#### EDIÇÃO

Directorate-General for Nuclear and Technological Development of the Navy - DGDNTM

[www.marinha.mil.br/dgdntm/revista](http://www.marinha.mil.br/dgdntm/revista)

#### EDITORIAL PRODUCTION

Zeppelini Publishers / Instituto Filantropia

[www.zeppelini.com.br](http://www.zeppelini.com.br)

#### EDITORIAL COMMISSION

Adriano Joaquim de Oliveira Cruz - UFRJ - Rio de Janeiro/RJ/Brazil

Aldebaro Barreto da Rocha Klautau Júnio - UFPA - Belém/PA/Brazil

Aletéia Patrícia Favacho de Araújo - UNB - Brasília/DF/Brazil

André Andrade Longaray - FURG - Rio Grande/RS/Brazil

Andre Luiz Lins de Aquino - UFAL - Maceió/AL/Brazil

Cintia de Moraes Borba - FIOCRUZ - Rio de Janeiro/RJ/Brazil

Genaina Nunes Rodrigues - UNB - Brasília/DF/Brazil

Giovane Quadrelli - UCP - Petrópolis/RJ/Brazil

Gilson Brito Alves de Lima - UFF - Rio de Janeiro/RJ/Brazil

Jaci Maria Bilhalva Saraiva - CENSIPAM - Brasília/DF/Brazil

José Maria Parente de Oliveira - ITA - São José dos Campos/SP/Brazil

José Mario De Martino - FEEC/UNICAMP - Campinas/SP/Brazil

Jose Manoel Seixas - UFRJ - Rio de Janeiro/RJ/Brazil

Luciano Zogbi Dias - FURG - Rio Grande/RS/Brazil

Maria Eveline de Castro Pereira - FIOCRUZ - Rio de Janeiro/RJ/Brazil

Marcos Evandro Cintra - UFERSA - Mossoró/RN/Brazil

Marcelo Sperle Dias - UERJ - Rio de Janeiro/RJ/Brazil

Mirian Enriqueta Bracco - UERJ - Rio de Janeiro/RJ/Brazil

Natanael Nunes de Moura - UFRJ - Rio de Janeiro/RJ/Brazil

Newton Narciso Pereira - USP - São Paulo/SP/Brazil

Nivaldo Silveira Ferreira - UENF - Campos dos Goytacazes/RJ/Brazil

Paulo Sérgio Soares Guimarães - UFMG - Belo Horizonte/MG/Brazil

Raul Francé Monteiro - PUC-Goiás - Goiânia/GO/Brazil

Ricardo Coutinho - IEAPM - Rio de Janeiro/RJ/Brazil

Thiago Pontin Tancredi - UFSC - Florianópolis/SC/Brazil

Vivian Resende - UFMG - Belo Horizonte/MG/Brazil

Walter Roberto Hernández Vergara - UFGD - Dourados/MS/Brazil

THE REVISTA PESQUISA NAVAL IS SPONSORED BY

FUNDAÇÃO CONRADO WESSEL

**FCW**

Revista Pesquisa Naval / Diretoria-Geral de Desenvolvimento Nuclear e Tecnológico da Marinha  
v. 1, n. 1, 1988 - Brasília - DF - Brasil - Marinha do Brasil

Anual

Título abreviado: Pesq. Nav.

ISSN Impresso 1414-8595 /

ISSN Eletrônico 2179-0655

1. Marinha - Periódico - Pesquisa Científica. Diretoria-Geral de Desenvolvimento Nuclear e Tecnológico da Marinha.

CDU 001.891.623/.9  
CDD 623.807.2

**1 PRESENTATION**

*Bento Costa Lima Leite de Albuquerque Junior*

**OPERATING ENVIRONMENT**

**2 A RISK CLASSIFICATION MODEL FOR ORGANIC AIRCRAFT OPERATIONS: A MULTIPLE CRITERIA APPROACH**

Modelo de classificação de risco para operações com aeronaves embarcadas: uma abordagem multicritério

*Luiz Fernando do Nascimento, Mischel Carmen Neyra Belderrain*

**13 THE OPERATIONAL RISK MANAGEMENT APPLIED TO THE SCIENTIFIC DEVELOPMENT OF "THE BLUE AMAZON" - AMAZÔNIA AZUL**

O gerenciamento do risco operacional aplicado ao desenvolvimento científico da Amazônia Azul

*Guilherme Pires Black Pereira*

**NAVAL ARCHITECTURE AND PLATFORM**

**21 INVESTIGATION ON STRUCTURAL RESPONSE, INDUCED BY SLAMMING EFFECT IN A MONOHULL SEMIDISPLACEMENT SHIP BY MEANS OF SUBSTRUCTURED MODELING**

Investigação sobre a resposta estrutural, induzida pela batida de proa em embarcação monocasco de semiplano, por meio de modelagem por subestruturação

*fabio da Rocha Alonso, Waldir Terra Pinto*

**HUMAN PERFORMANCE AND HEALTH**

**34 ACCIDENTS WITH WATERWAY TRANSPORTS DUE TO EXTREME WEATHER CONDITIONS**

Acidentes com transportes hidroviários em ocasião de extremos meteorológicos

*Suanne Honorina Martins dos Santos, Maria Isabel Vitorino, Jefferson Inayan de Oliveira Souto, Edson José Paulino da Rocha*

**DECISION-MAKING PROCESS**

**45 LITHOLOGY DISCRIMINATION BY SEISMIC ELASTIC PATTERNS: A GENETIC FUZZY SYSTEMS APPROACH**

Discriminação litológica por atributos sísmicos elásticos: uma abordagem por sistemas fuzzy-genéticos

*Eric da Silva Praxedes, Adriano Soares Koshiyama, Marley Maria Bernardes Rebuzzzi Vellasco, Marco Aurélio Cavalcanti Pacheco, Ricardo Tanscheit*

**SENSORS, ELECTRONIC WARFARE AND ACOUSTIC WARFARE**

**57 COMPARISON BETWEEN THE THEORETICAL ESTIMATION AND THE MEASUREMENTS OF THE MAIN FIGURES OF MERIT OF QUANTUM WELL INFRARED PHOTODETECTORS**

Comparação entre a estimativa teórica e as medidas das principais figuras de mérito de fotodetectores infravermelhos a poços quânticos

*Ali Kamel Issmael Junior, Fábio Durante Pereira Alves, Ricardo Augusto Tavares Santos*

---

**71 BLIND AND ASSISTED SIGNAL DETECTION FOR UWB SYSTEMS  
BASED ON THE IEEE 802.15.4A STANDARD**

Detecção cega e assistida de sinais em sistemas UWB baseados no padrão IEEE 802.15.4A

*Aline de Oliveira Ferreira, Cesar Augusto Medina Sotomayor, Fabian David Backx,  
Raimundo Sampaio Neto*

**82 BRAZILIAN PASSIVE SONAR: ADVANCES AND TECHNOLOGY  
SHOWCASE**

Sonar passivo nacional: avanços e demonstração de tecnologia

*Fabricio de Abreu Bozzi, William Soares Filho, Fernando de Souza Pereira Monteiro,  
Carlos Alfredo Órfão Martins, Gustavo Augusto Mascarenhas Goltz,  
Orlando de Jesus Ribeiro Afonso, Cleide Vital da Silva Rodrigues,  
Fernando Luiz de Magalhães, Leonardo Martins Barreira*

**INFORMATION AND COMMUNICATIONS TECHNOLOGY**

**93 AN ARCHITECTURE TO MANAGE SOFTWARE ENGINEERING PROJECTS  
AIMED AT INTEGRATION WITHIN THE BRAZILIAN ARMED FORCES**

Uma arquitetura para a gestão dos projetos de engenharia de *software* visando à integração nas Forças Armadas

*Geraldo da Silva Souza, Rodrigo Abrunhosa Collazo, Jones de Oliveira Avelino,  
Carlos Eduardo Barbosa*

## PRESENTATION

The Navy, over time, has been a leader in the area of Science, Technology, and Innovation (ST&I), with results that go beyond the Navy Force, generating achievements and benefits for the country. The pioneering spirit of Admiral Álvaro Alberto da Mota e Silva, patron of the Navy's ST&I and a Brazilian scientist, stands out. He dreamed up and implemented the National Nuclear Energy Commission (CNEN) and the National Council for Scientific and Technological Development (CNPq) in the 1950s, and was its first president.

The Naval Force has always sought to improve itself. With its legacy achieved in the area of ST&I as its guide until today, it changed its organizational structure. It changed the name of the Secretary of Science, Technology and Innovation of the Navy, SecCTM, to the Board of Directors of Nuclear and Technological Development of the Navy (DGDNTM). It is the responsibility of the Board of Directors to plan, organize, direct, and control all of the Navy's ST&I activities, including the relevant Submarine Development Program (PROSUB) and the Navy's Nuclear Program (PNM).

These programs, which will allow Brazil to obtain its first nuclear powered submarine thorough design and construction, have shown that the benefits derived from the Naval Force's ST&I investments continue to go beyond the exclusive area of the Navy. Its beneficiaries include the areas of electric power generation and health, because, in partnership with the Nuclear Industries of Brazil (INB) and the Nuclear and Energy Research Institute (IPEN), we are working on achieving Brazilian autonomy in the production of nuclear fuel for the nuclear power plants in Angra dos Reis (RJ) and in the implementation of the the

Brazilian Multipurpose Reactor (RMB), which will produce radiopharmaceuticals.

The demand for new technologies has led the Navy to establish new Strategic Partnerships with the academic and business sectors, as well as with other governmental institutions, as it guides the concept of innovation known as the Triple Helix. Some legal documents of cooperation have already been signed and cooperation are being expanded with activities drawing on mutual knowledge, such as workshops and symposia with several institutions in different regions of Brazil.

In this context, the Naval Research Journal has, since its first edition in 1988, made a relevant contribution to the dissemination of the Navy's CT & I activities, and is therefore an important instrument for interaction with the academic and business sectors and with other governmental bodies. As I present a new collection of scientific articles, I take this opportunity to salute all those who, in some way, have collaborated to achieve this level of scientific and technological development. Bravo Zulu!

Pleasant reading!



**BENTO COSTA LIMA LEITE DE ALBUQUERQUE JUNIOR**  
Fleet Admiral  
Director General of Nuclear and Technological  
Development of the Navy

# COMPARISON BETWEEN THE THEORETICAL ESTIMATION AND THE MEASUREMENTS OF THE MAIN FIGURES OF MERIT OF QUANTUM WELL INFRARED PHOTODETECTORS

Comparaç o entre a estimac o te rica e as medidas das principais figuras de m rito de fotodetectores infravermelhos a po os qu nticos

Ali Kamel Issmael Junior<sup>1</sup>, F bio Durante Pereira Alves<sup>2</sup>,  
Ricardo Augusto Tavares Santos<sup>3</sup>

**Abstract:** This paper presents a comparison between the theoretical estimation and the measures of the main figures of merit of quantum well infrared photodetectors (QWIP). Mathematical models of the main figures of merit such as absorption coefficient, dark current, and responsivity, available in the specialized literature, are analyzed, compared, and implemented in MatLab<sup>®</sup>. The results of numerical simulations are compared with experimental data published in other studies and show that the models which are properly adapted have great potential for use in projects of real devices.

**Keywords:** Photodetectors. Quantum Wells. Characterization. Military Applications.

**Resumo:** Este artigo traz uma discuss o da compara o entre estimac o te rica e medidas das principais figuras de m rito de fotodetectores infravermelhos a po os qu nticos (QWIP). Modelos matem ticos do coeficiente de absorc o, da corrente de escuro e da responsividade, dispon veis na literatura especializada, s o analisados, comparados e implementados utilizando a ferramenta computacional MatLab<sup>®</sup>. Os resultados das simula es s o comparados com dados experimentais publicados em outros estudos e indicam que os modelos, convenientemente adaptados, apresentam grande potencialidade para serem utilizados em projetos de dispositivos reais.

**Palavras-chaves:** Fotodetectores. Po os Qu nticos. Caracteriza o. Aplica es Militares.

## 1. INTRODUCTION

Photodetection is now a technological reality that has increased the possibilities in several fields of knowledge. One of them is Defense, since the characterization of

objects or scenes by photodetectors with high sensitivity and selectivity in a wide infrared spectral range enables systems – such as missile guidance ones – to obtain more accuracy in the selection and hitting of a target.

**1.** Bachelor's degree in Electrical Engineering, with emphasis on Electronic Systems (1999), at "Universidade do Estado do Rio de Janeiro" (UERJ), Brazilian Navy Engineer Officer (since 2000) and expert in Electromagnetic Environment's Analysis (2007), at "Instituto Tecnol gico de Aeron utica" (ITA). He is currently an Assistant for the Management of the S-BR Combat System Development, in the "Coordenadoria-Geral do Programa de Desenvolvimento do Submarino com Propuls o Nuclear" (COGESN), Rio de Janeiro, RJ - Brazil. E-mail: ali.kamel@marinha.mil.br and alikamel@ig.com.br

**2.** Bachelor's degree in Aeronautical Sciences (1986) at "Academia da Forc a A rea" (AFA). Graduated in Electrical Engineering (1997) at "Instituto Tecnol gico de Aeron utica" (ITA). Master's degree in Electrical Engineering and Computer Science (1998) at "Instituto Tecnol gico de Aeron utica" (ITA). Master's degree in Electrical Engineering at the Naval Postgraduate School (NPS) - USA (2006), Electrical Engineering degree at the Naval Postgraduate School - USA (2007). PhD in Physics (2008) at "Instituto Tecnol gico de Aeron utica" (ITA) and Postdoctoral researcher in the field of Terahertz detector arrays at the Naval Postgraduate School (NPS) - USA (2011). He is currently the Air Force Reserve Colonel in the "Forc a A rea Brasileira" (FAB), Associated researcher at the Physics Department of the Naval Postgraduate School (NPS) and Collaborating Professor (volunteer) at the Electronic Engineering Division at "Instituto Tecnol gico de Aeron utica" (ITA) - S o Jos  dos Campos, SP - Brazil. E-mail: durante@ita.br

**3.** Graduated in Aeronautical Sciences and Military Pilot at the Academia da Forc a A rea (AFA) in 1993. In 2001, he specialized in Electromagnetic Environment's Analysis and obtained a Master's degree in Electrical Engineering and Computer Science (2004) at "Instituto Tecnol gico de Aeron utica" (ITA). In 2009, he concluded the doctoral program also at "Instituto Tecnol gico de Aeron utica" (ITA). He is currently the Deputy Director of Operational Evaluation and Research and Development of the "N cleo do Instituto de Aplica es Operacionais" (NuIAOp) of the "Comando-Geral de Opera es A reas" (COMGAR), in S o Jos  dos Campos, SP - Brazil E-mail: tavares.ricardoaugusto@gmail.com

Infrared radiation comes from the molecular agitation caused by the high temperatures of bodies and objects. More precisely, all bodies above the absolute zero emit radiation. Figure 1 (NASA, 2007) shows the location of infrared radiation inside the electromagnetic spectrum.

The infrared region of the electromagnetic spectrum, depending on the reference used, can be subdivided into four bands: near infrared (NIR), between 0.7 and 3.0  $\mu\text{m}$ ; mid-wavelength infrared (MIR), between 3.0 and 6.0  $\mu\text{m}$ ; long-wavelength infrared (LWIR), between 6.0 and 15.0  $\mu\text{m}$ ;

and very long-wavelength infrared (VLWIR), whose wavelength was higher than 15.0  $\mu\text{m}$  (ALVES, 2005). These subdivisions can be visualized in Table 1.

The atmosphere, where radiation is propagated, is composed of gas and suspended particles distributed through different temperatures and pressure, defined by altitude and geographic position. The gas and the particles can be placed in six different layers distributed according to the altitude variation. The lowest one – usually the scenario used in military applications – is the troposphere, which extends from

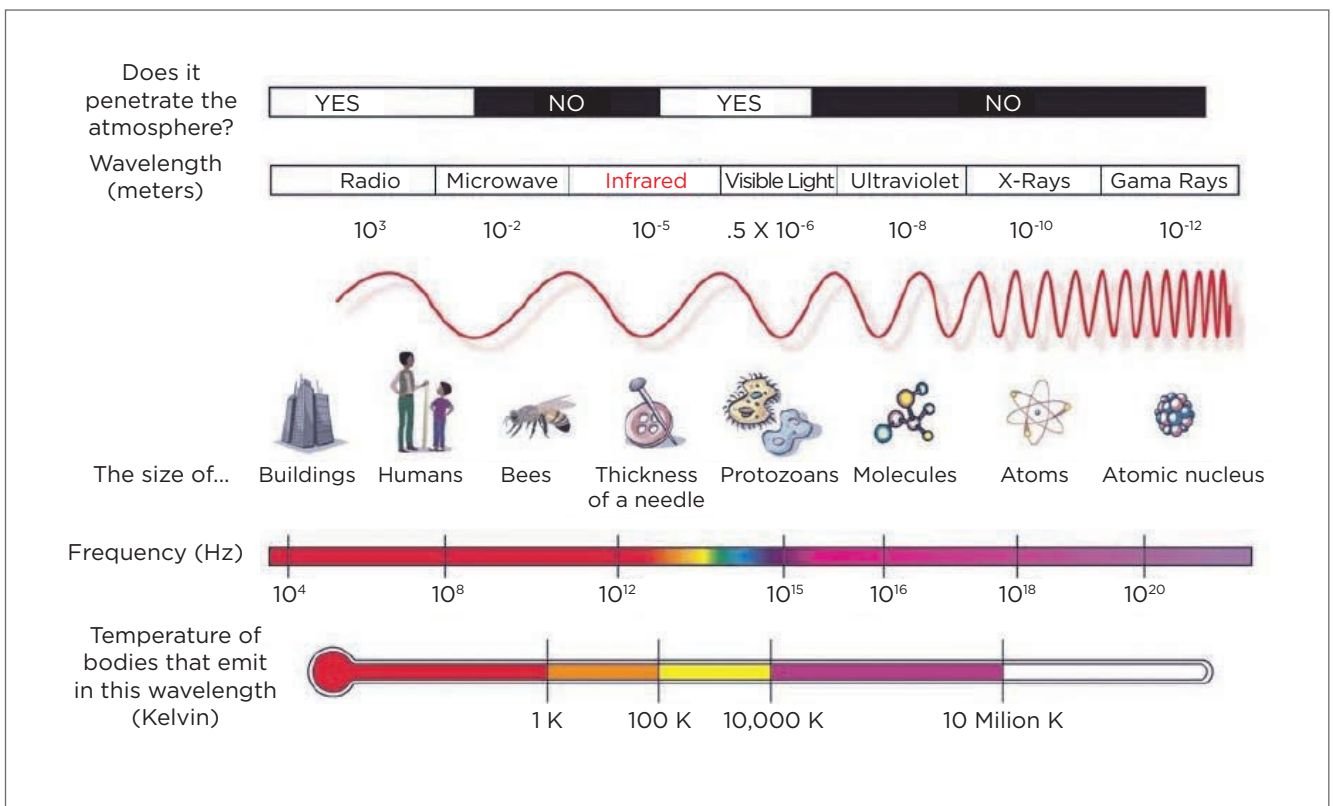


Figure 1. The electromagnetic spectrum and the location of infrared radiation (NASA, 2007).

Table 1. Subdivisions of infrared radiation band (ALVES, 2005).

Name	Abbreviation	Limits ( $\mu\text{m}$ )
Near infrared	NIR	0.75 to 3
Mid-wavelength infrared	MIR	3 to 6
Long-wavelength infrared	LWIR	6 to 15
Very long-wavelength infrared	VLWIR	15 a 1000

sea level to approximately 11 km (SANTOS, 2004), depending on the season and the latitude. In this layer, temperature falls whereas altitude rises, in a 6.5 K/km ratio; however, this ratio may change, and that can cause scattering effects (SANTOS, 2004). Infrared radiation attenuation mostly occurs in this layer, and its main components are water, carbon dioxide, clouds, and smoke. The other layers are stratosphere, mesosphere, ionosphere, thermosphere, and exosphere. When infrared is transmitted through the atmosphere, the gases make a selective absorption, and scattering is provoked by the suspended particles. Sometimes, there is some modulation caused by quick changes in temperature and/or pressure.

Water steam is a major attenuation factor for optical radiation, and it is prevalent in altitudes lower than 10 km. Attenuation above this level is despicable. Carbon dioxide is present until 5 km, approximately, and it only attenuates infrared radiation. Considering the attenuation effects of

the atmosphere, infrared detectors are designed to respond to frequency bands in which infrared radiation transmittance is maximum. Figure 2 shows that atmospheric transmittance limits the possibility of detection in three well-defined regions: 0.7–2.5  $\mu\text{m}$ , 3.0–5.0  $\mu\text{m}$ , and 8.0–15.0  $\mu\text{m}$ , therefore corresponding to bands NIR, MIR, and LWIR, respectively (BOSCHETTI, 2015).

In this context, quantum well infrared photodetectors (QWIP) have become a good choice for modern photodetection systems. In the case of military applications, there is a demand for detectors with special features to be used in the battlefield, in missions that might involve target recognition, environment imaging, or fields of interest – besides missile guidance. QWIP cameras are very attractive for this application because of its high selectivity and multispectral detection characteristics, enabling the detection and identification through high-resolution images (GUNAPALA et al., 2007; GUNAPALA, 2007; DYER; TIDROW, 1998).

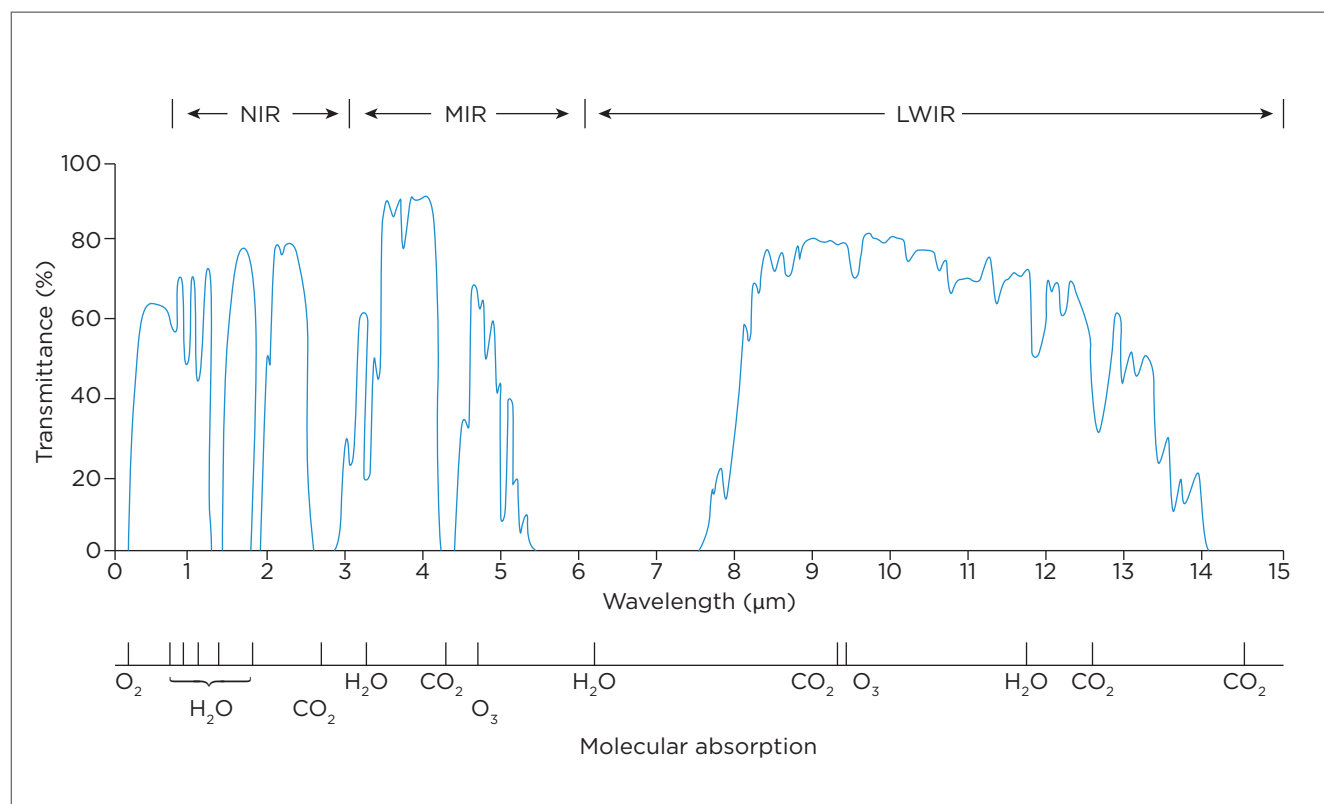


**Figure 2.** Atmospheric transmission spectrum, in the near, mid- and long-wavelength infrared bands. The spectrum corresponds to a layer of 1830 m of air at sea level, with 40% of relative humidity at 25°C. The bottom of the figure shows the lines of absorption of some components in the atmosphere, responsible for the transmission curve (BOSCHETTI, 2015).

Since they generate wide infrared spectral range images – 6–20  $\mu\text{m}$  – (GUNAPALA, 2007), with high discriminatory power – 640  $\times$  512 lines – (GUNAPALA, 2007) in more than one band simultaneously and at a significantly low cost (GUNAPALA, 2007) – these systems are a good option for use in infrared-guided weapons (DYER; TIDROW 1998). With the significant and increasing lethal power of these war systems, such technology becomes a factor that generates asymmetry for the Armed Forces employing it. Figure 3 presents some products in the market that already use this technology.

The knowledge about the characteristics of construction of the QWIP and its performance evaluation factors technically subsidizes future acquisitions of devices, and increases the chances of carrying out the project, its development and manufacture in Brazil. Besides, the study of figures of merit and the development of mathematical tools that simulate it speed up the process of development, with reduced costs. This fact contributes with the technological independence in defense systems.

The results presented in this paper are part of a line of analysis research and development of quantum well photodetectors with capacity of simultaneous detection in three infrared bands: NIR, MWIR, and LWIR. This study has been performed with “Laboratório de Guerra Eletrônica”

(LabGE), “Instituto de Tecnologia de Aeronáutica” (ITA), the Sensor Research Laboratory (SRL), at the Naval Postgraduate School (NPS), in USA, and the National Research Council (NRC), in Canada. The results, published by Alves (2005), Hanson (2006), Alves et al. (2006), Issmael Jr. et al. (2007), Issmael Jr. (2007), and Alves et al. (2008), show the great potential of these devices for military applications. The production of quantum well photodetectors requires:

- Modeling the structures of semiconductor materials;
- Simulating and adjusting the figures of merit within the project requirements;
- Increasing the crystalline structure, characterizing it and repeating the process, after adjusting it to the models and the techniques of simulation;
- Fabricating detectors/cameras; and
- Analyzing the performance.

This cycle can be repeated several times, until the techniques of the project and the models are refined enough to be repetitive, according to some characteristics. In this context, being limited to quantum wells sensitive to LWIR, this paper shows the analysis of some models available in the literature for the main figures of merit, absorption coefficient, dark current, and responsivity. It shows the results obtained by the simulations performed with MatLab® – version

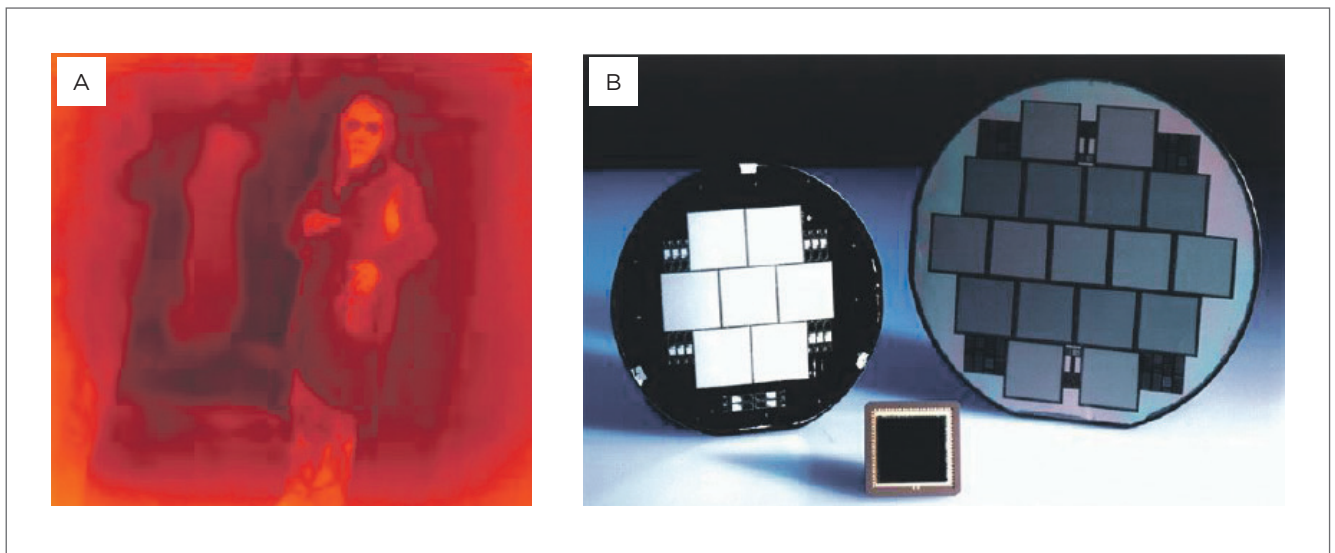


**Figure 3.** (A) Infrared image generated by a camera with quantum well infrared photodetectors (INOVAÇÃO TECNOLÓGICA, 2006); and (B) matrix of quantum well infrared photodetectors used for ballistic missile defense sensors (MISSILE DEFENSE AGENCE, 2007).

R2006b – from these models, and compares the results aiming at improving the models and their use. The importance of using MatLab® – besides its excellent performance, approved in studies of Engineering simulation – is owed to the fact that previous studies in this project were also conducted with it, so, there is no justification for the adaptation of other tools. This simplified the evolution of simulation routines in previous studies to obtain the results presented in this article.

## 2. METHODOLOGY

The denomination quantum well comes from potential well, which can be obtained when a semiconductor material is “grown” between two other semiconductors

– “sandwiched” –, with a larger energy gap, thus causing the formation of quantum energy levels, confining carriers in two dimensions. In this sense, infrared radiation can be absorbed, leading to excited carriers, so they go from a ground state to a higher state. When transition occurs between quantum levels inside the same band, it is called intersubband, and when it takes place between quantum levels, between the valence and conduction bands, is called interband. Figure 4 shows a diagram of bands in a quantum well-like structure. As observed in this figure, in intersubband transitions the energy transition is lower, enabling detection in the LWIR band – focus of this paper.

By selecting the material and controlling its composition and dimensions, the absorption spectrum, as well as

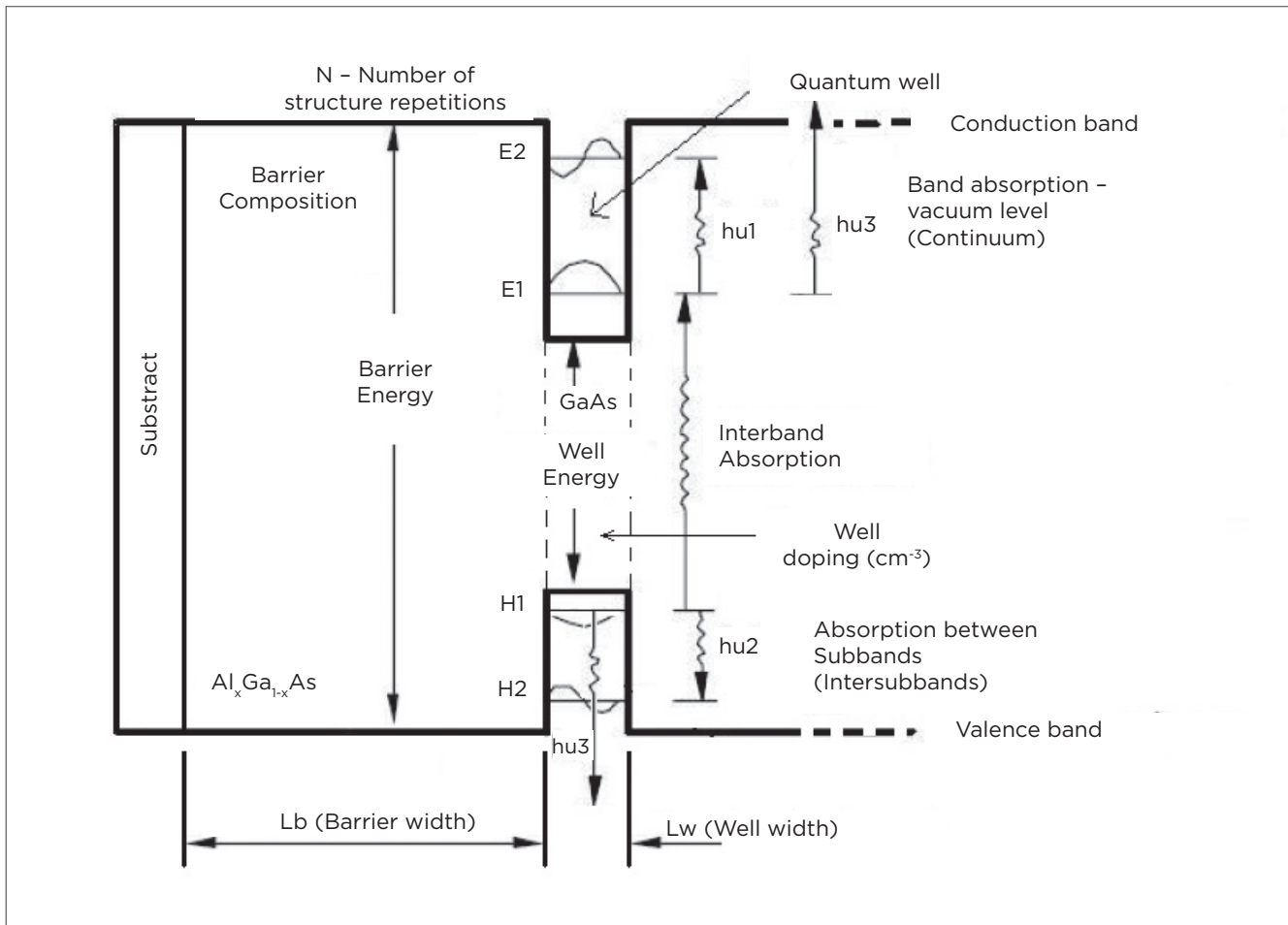


**Figure 4.** Band diagram, transitions between energy levels and the main building variables of a symmetric quantum well (ISSMAEL JUNIOR, 2007).

the other figures of merit, can be estimated. Therefore, we selected models available in the literature that could adequately describe the quantum phenomena of structures such as the one demonstrated in Figure 4, allowing the calculation of quantum energy levels, as well as the other parameters required to characterize the detectors. Structures reported in the literature were simulated in order to allow the validation of the models that were used to predict the features measured in a laboratory.

Table 2 presents the data from the samples used in simulations, all with wells composed of GaAs.

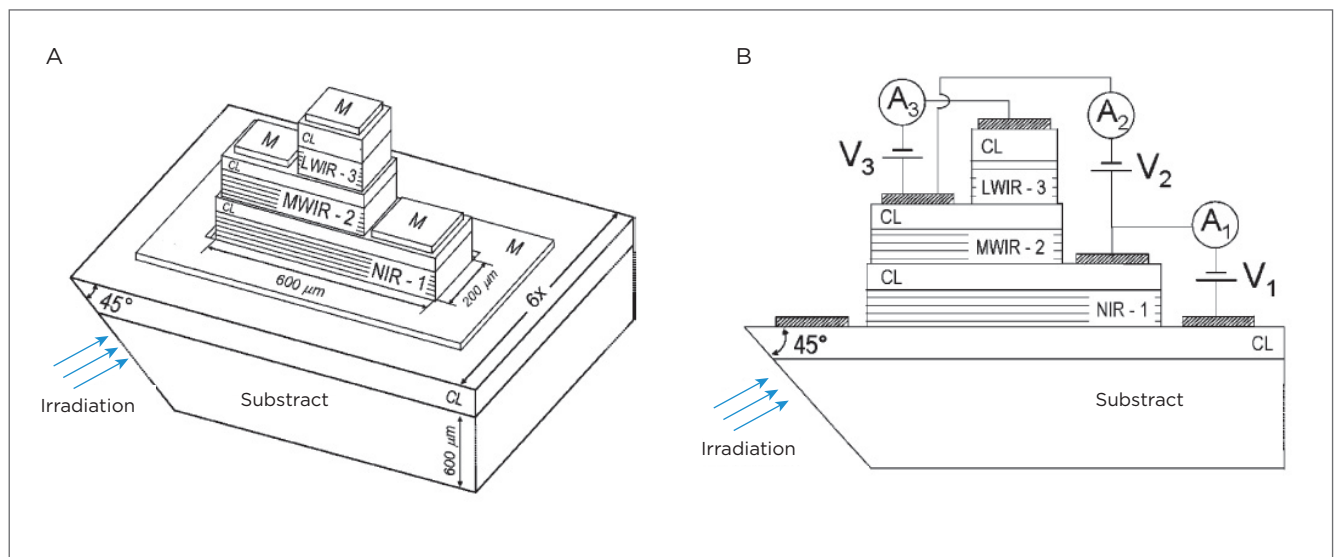
Figure 5 shows the multilayer photodetector and its polarization, which was built (ALVES, 2005) and is the base of the analysis of sample A.

Figure 6 (ALVES, 2005) presents the diagram of energy bands in sample A.

Figure 7 (ALVES, 2005) shows the image of the photodetector in sample A.

**Table 2.** Samples used in the simulations.

Sample	Reference	Barrier width (Lb) (ångström)	Well width (Lp) (ångström)	Barrier composition	Number of repetitions	Well doping (cm <sup>-3</sup> )
A	(ALVES, 2005) Page. 62	300	52	Al <sub>0,26</sub> Ga <sub>0,74</sub> As	20	0.5.10 <sup>18</sup>
B	(LEVINE, 1993) Page. R22 and R29 and (GUNAPALA e BANDARA, 1999) Pages. 23 and 34	500	40	Al <sub>0,26</sub> Ga <sub>0,74</sub> As	50	1.10 <sup>18</sup>
C	(LEVINE, 1993) Pages. R22 and R29	500	50	Al <sub>0,26</sub> Ga <sub>0,74</sub> As	25	0.42.10 <sup>18</sup>
D	(LEVINE, 1993) Page R18	305	40	Al <sub>0,29</sub> Ga <sub>0,71</sub> As	50	1.4.10 <sup>18</sup>



**Figure 5.** (A) Tridimensional Diagram of the multilayer detection device and (B) vertical cut of the device, emphasizing the independent building configuration of each layer associated with an infrared spectrum detection band (ALVES, 2005).

Figure 8 has the diagram of bands in the samples listed in Table 2.

First, we calculate the potential profile of the structures, considering that the dimensions in the growth axis  $z$  are several orders of magnitude lower than in plan  $x$ - $y$ , restricting the unidimensional confinement of the carriers – electrons in the conduction band and holes in the valence band. The potential is basically determined by the band offset in the interface, by the external electric field applied on the structure and by the distribution of charges. The first is obtained from parameters reported in the literature and empirical adjustments obtained in the laboratory. The second is known and controlled by the device user. The third requires knowledge of the confined energy levels, as well as their respective wave functions; in this case, the Schrodinger–Poisson equations must be solved in a self-consistent manner (ALVES, 2005). In order to solve differential equations and obtain eigenvalues and

eigenfunctions, Alves (2005) used the Shooting method (HARRISON, 2005) due to its versatility to calculate

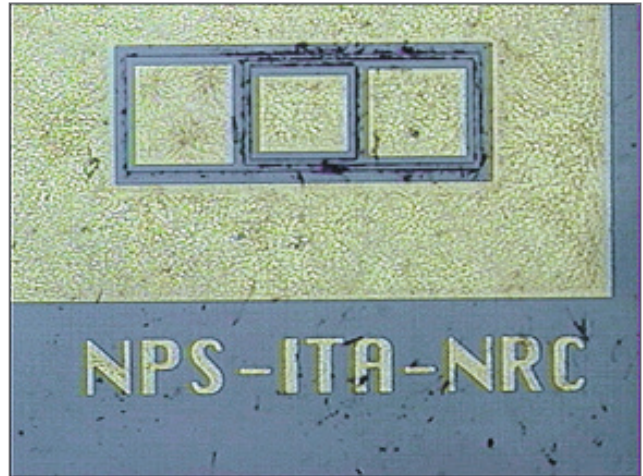


Figure 7. Image of the photodetector in sample A (ALVES, 2005).

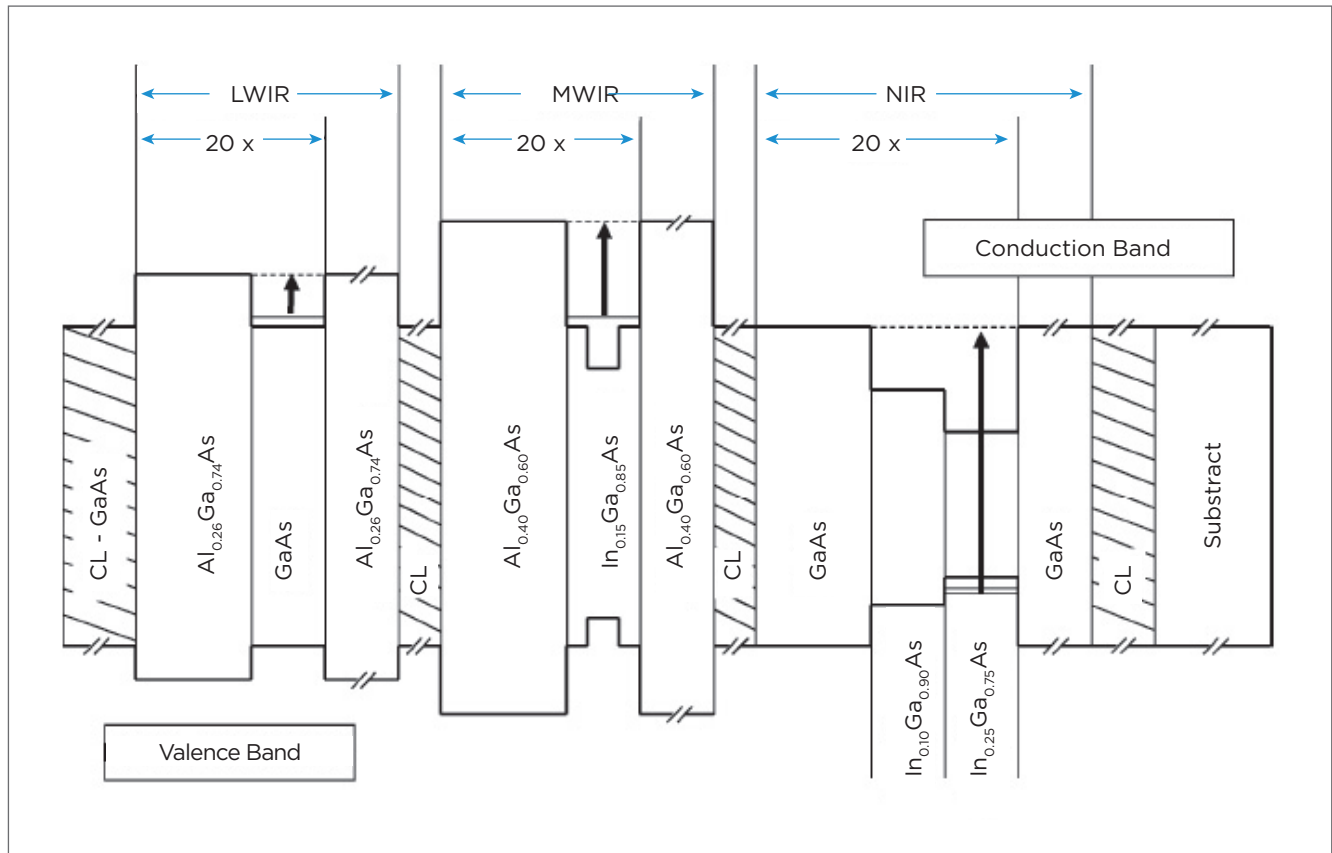


Figure 6. Diagram of the energy bands of 3-band quantum well infrared photodetectors. The width of each layer was not drawn in scale (ALVES, 2005).

complex structures. Next, equations that shape figures of merit are solved and detailed in the next section.

Experimental data to be compared with the simulations of A were obtained from measurements described in the study by Alves (2005), whereas the other samples were extracted directly from the graphs available in previously mentioned references – using the graph tool GraphData 1.0<sup>®</sup> – and the analyses – using the *software* Origin<sup>®</sup>.

### 3. RESULTS

#### 3.1. ABSORPTION SPECTRUM

The absorption spectrum represents the main characteristic of the crystalline structure sample, allowing its evaluation before the detector itself is manufactured. It indicates the band of operation of the detector and the type of quantum transition resulting from the interaction between photon and electron. The theoretical estimation of this spectrum can be obtained by Equations 1 and 2 (ALVES, 2005):

$$\alpha_{CbCb}(\hbar\omega) = \frac{q^2 d}{(m_e^*)^2 \epsilon_0 n_r c(\hbar\omega)} \left| \Psi_{\beta}(z) \right| \left| \frac{\partial}{\partial z} \Psi(z) \right|^2 X \cos^2 \varnothing \frac{\Gamma}{(E_{\beta} - E - \hbar\omega)^2 + (\Gamma/2)^2} \quad (1)$$

In which  $\alpha_{CbCb}$  is the absorption coefficient, considering transitions between the confined levels in the conduction band (bound-to-bound);  $d$  is the doping density;  $E_i$  and  $E_f$  represent the initial and final energy levels, respectively;  $q$  is the electron charge;  $c$  is the speed of light in the vacuum;  $\epsilon_0$  is the vacuum electric permittivity;  $\Gamma$  is the broadening parameter;  $\omega$  is the incident photon energy;  $m_e^*$  is the effective electron mass; and  $\varnothing$  is the angle between the incident flow and the growth axis.

$$\alpha_{CbC}(\hbar\omega) = \frac{q^2 d}{(m_e^*)^2 \epsilon_0 n_r c(\hbar\omega)} \frac{L_{fp}}{\pi} \sqrt{\frac{m_{e,b}^*}{2(E_f - V_o)}} X \left| \Psi_{\beta}(z) \right| \left| \frac{\partial}{\partial z} \Psi(z) \right|^2 X \cos^2(\varnothing) \quad (2)$$

In which  $\alpha_{CbC}$  is the absorption coefficient, considering transitions between one confined level and continuum levels in the conduction band;  $L_{fp}$  is the ratio between  $p$  and the wave vector  $k_{Lfp}$ ; and  $V_o$  is the barrier energy.

The characteristics of the sample are listed in Table 2. The parameters required to solve (1) and (2) are extracted from Vurgaftman and Meyer (2001). Therefore, the absorption spectrums of samples A and B were estimated for the temperature of 300 K. Amplitude absolute values presented differences in magnitude orders. This fact is owed to the

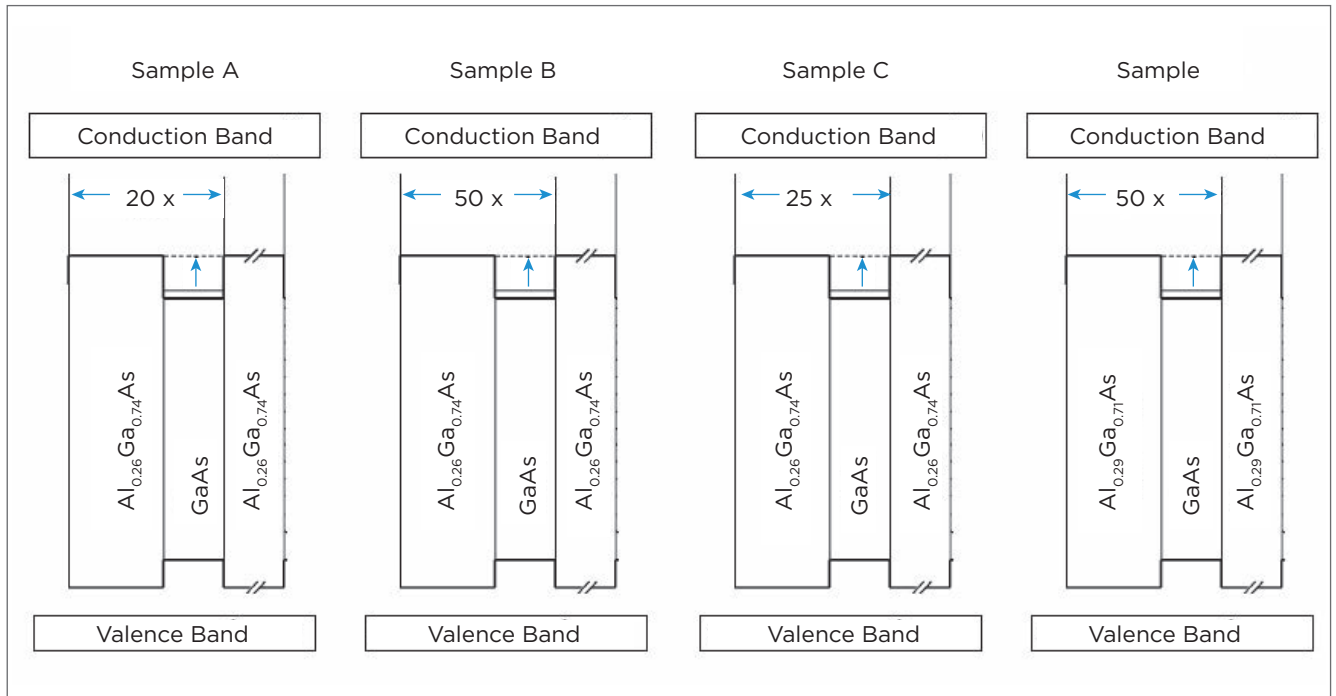


**Figure 8.** Diagram of the energy bands of photodetectors used in the simulations. The width of each layer was not draw in scale.

large number of uncertainties in the parameters of semiconductor materials composing the structure of the samples (VURGAFTMAN; MEYER, 2001). So, at the time of simulations, the priority was to determine the wavelength at the peak, without considering the broadening coefficient because of the aforementioned inaccuracy. When the absorption coefficient is normalized (Figure 9), good estimation is obtained, with errors lower than 6.03% for the wavelength at the peak. This shows that the calculation of confined levels using the shooting method is very reasonable.

### 3.2. DARK CURRENT

The dark current is the figure of merit that represents how much current is generated in the photodetector without the influence of incident radiation (that is, in the dark). Three mechanisms of dark current generation can be identified in quantum well devices: sequential resonant tunneling, temperature-assisted tunneling and thermionic effect. The calculation of the dark current is a complex procedure that depends on several magnitudes. The first magnitude to be calculated is the effective weighted mass of the electron in the detector, from the proportion of barriers and wells in the detector. The procedure is carried out by determining the effective masses of the electron in the barrier (FU; WILLANDER, 1998) – formed by the ternary composition AlGaAs from the binary compositions GaAs and AlAs – and in the well – formed only by the binary composition GaAs. The second magnitude is the weighted carrier mobility, which

is also obtained from the mobility in the barrier and in the well. The third magnitude is the velocity weighted saturation in the detector. These parameters were obtained considering the models from the Institute of Microelectronics's Site (2014). More details in Issmael Junior (2007).

One of the ways of presenting the dark current in QWIP is given by Equation 3 (LEVINE, 1993):

$$I_D(F) = \frac{e \cdot v_{drift} \cdot A \cdot m_w^*}{\pi \hbar^2 L} \int_{E_i}^{\infty} f^{FD}(E) \cdot T(E, F) dE \quad (3)$$

In which the term outside the integral is the density of states divided by the period of the multiple quantum wells ( $L$ ), and the term  $f^{FD}(E)$  represents the Fermi-Dirac distribution, given by Equation 4 (ALVES, 2005):

$$f^{FD}(E) = \frac{1}{1 + e^{\frac{E - E_F}{k_B T}}} \quad (4)$$

In which  $E_F$  represents the level of bidimensional Fermi,  $k_B$  is the Boltzmann constant, and  $T$  is temperature. The tunneling coefficient –  $T(E, F)$  – depends on the polarization voltage and, for a simple barrier, it can be represented by the Equations 5, 6 and 7 (ANDREWS; MILLER, 1991):

$$T(E, F) = \exp \left[ -\frac{4L_b}{3qV} \left( \frac{2m^*}{\hbar} \right)^{1/2} \left[ (V_o - E)^{3/2} - (V_o - E - qV)^{3/2} \right] \right] \quad (5)$$

for  $E_o < E < V_o - qV$ ;

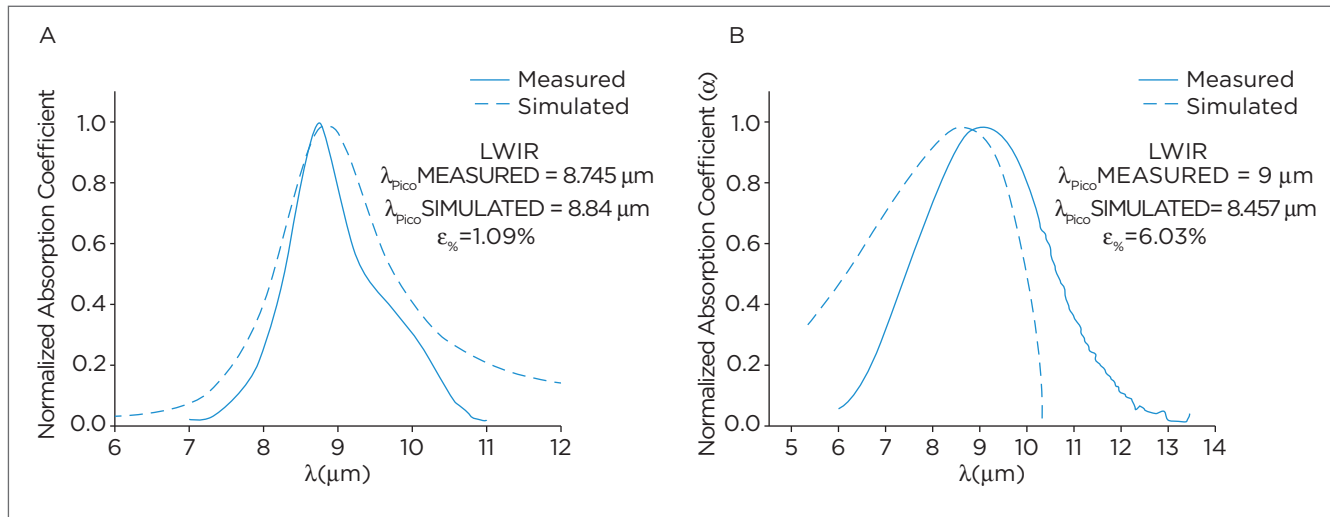


**Figure 9.** Comparison between estimated and measured values of the normalized absorption coefficient (A) in sample A (ALVES, 2005) and (B) in sample B (GUNAPALA; BANDARA, 1999).

$$T(E, F) = \exp \left( - \frac{4L_b \left( \frac{2m^*}{\hbar} \right)^{\frac{1}{2}} \left[ (V_o - E)^{3/2} \right]}{3qV} \right) \quad (6)$$

for  $V_o - qV < E < V_o$ ; e

$$T(E, F) = 1 \quad (7)$$

for  $E > V_o$ .  
 $V$  represents the voltage applied per period of well structure. In the case of electrons, the drift velocity ( $v_{drift}$ ) in function of the  $F$  field is given by Equation 8 (ALVES, 2005):

$$v_{drift} = \frac{\mu F}{\sqrt{1 + \left( \frac{\mu F}{v_{sat}} \right)^2}} \quad (8)$$

Using the mobility values ( $m$ ) equal to  $0.1 \text{ m}^2/\text{Vs}$  and the saturation velocity ( $v_{sat}$ ) equals to constant  $5.10^4 \text{ m/s}$ , the dark current was estimated for sample D (Table 1). The theoretical values presented a systematic error of 9% for all

temperatures. With this correction, we reach the result in Figure 10. Temperatures lower than 50 K are poorly represented by this model and were not included in the figure.

The models give a good representation of the phenomena, being a little bit further for values of polarization voltage lower than 1.0 V.

Then, the results in sample A (Table 1) were compared for temperatures 100, 90, 80, 77, 70, 60, 50, and 40 K. The correction factor was not applied for this structure, and the absolute values are presented in Figure 11.

The theory represents well the behavior of the real device for temperatures above 60 K and polarization voltage greater than 1.0 V, for the simplified criteria we considered. The discrepancies observed can be caused by several reasons, such as the fact that the configuration of the detector is part of a multilayer device, in which the NIR and MWIR layers can interfere in the measurements, and the increasing chances of tunneling induced by the external electrical field. Further studies should be conducted to obtain a single and generic

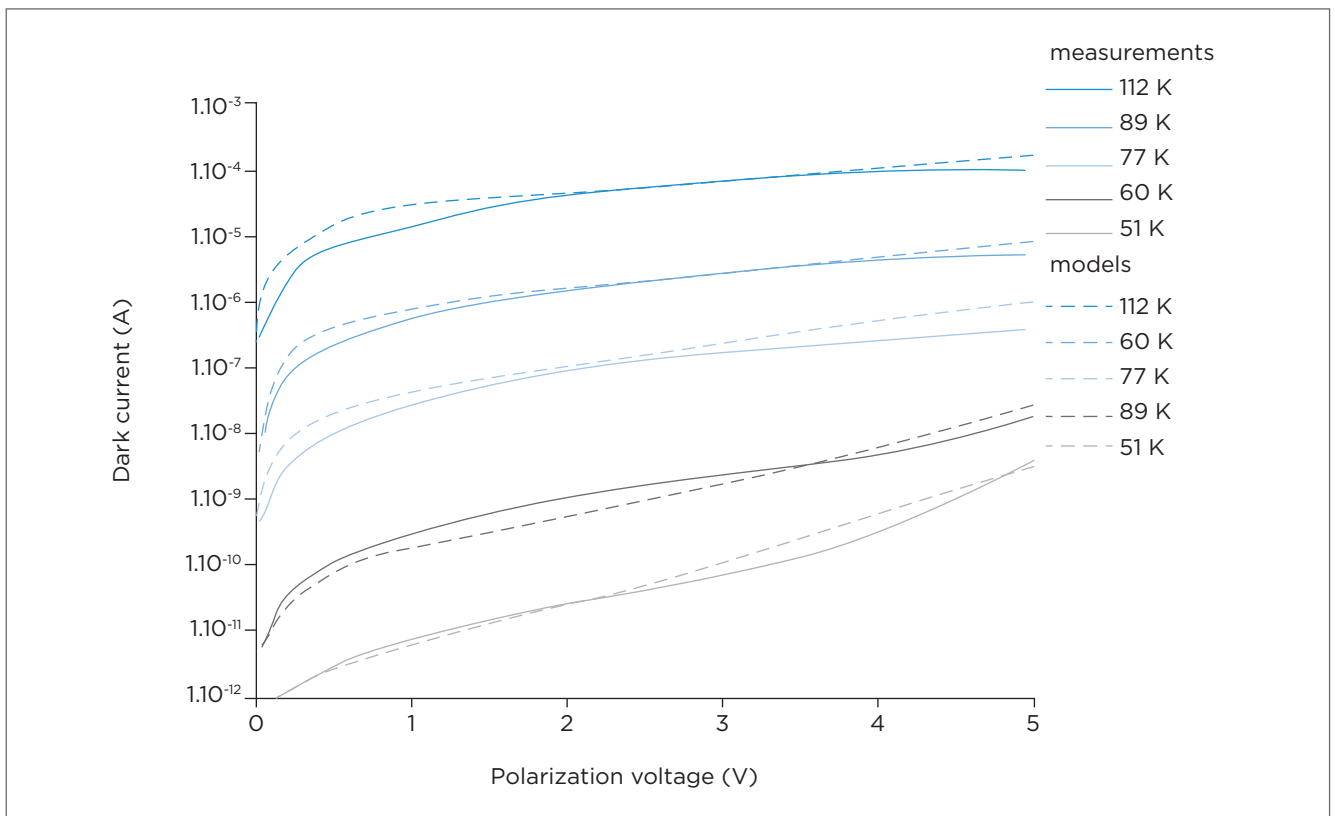


**Figure 10.** Comparison between the curves  $I \times V$  in the dark for sample D in Table with, with constant mobility and velocity saturation (ISSMAEL JUNIOR, 2007).

model. Since we did not have the detector of sample A at the time of simulations, it was not possible to take measurements with negative and positive polarization, which would allow a more accurate comparison and analysis with the result obtained.

### 3.3. RESPONSIVITY

Responsivity quantifies the photocurrent ratio generated by the photon radiation power incident in the detector. Mathematically is given by Equation 9 (ALVES, 2005):

$$R(F) = \frac{I_p(F)}{\Phi_o} \tag{9}$$

In which,  $I_p(F)$  is the photocurrent and  $F_o$  is the incident optical power.

The photocurrent can be expressed by Equation 10 (ALVES, 2005):

$$I_p(F) \approx \frac{2q\Phi_o}{\hbar\omega} \alpha L_w \sum_{n=1}^N e^{\frac{nL}{v_{drift}(F)\tau}} \tag{10}$$

In which  $\alpha$  is the absorption coefficient,  $\Phi_o$  is the incident optical power,  $\hbar\omega$  is the photon energy,  $q$  is the electron charge,  $L$  is the repetition period well/barrier,  $L_w$  is the width of the well,  $v(F)$  is the drift velocity of electrons influenced by the electrical field  $F$ ,  $e$   $\tau$  lifespan of the carrier extracted from the well. By combining these two expressions, we obtain the following Equation 11:

$$R_p(F) \approx \frac{2q}{\hbar\omega} \alpha L_w \sum_{n=1}^N e^{\frac{nL}{v_{drift}(F)\tau}} \tag{11}$$

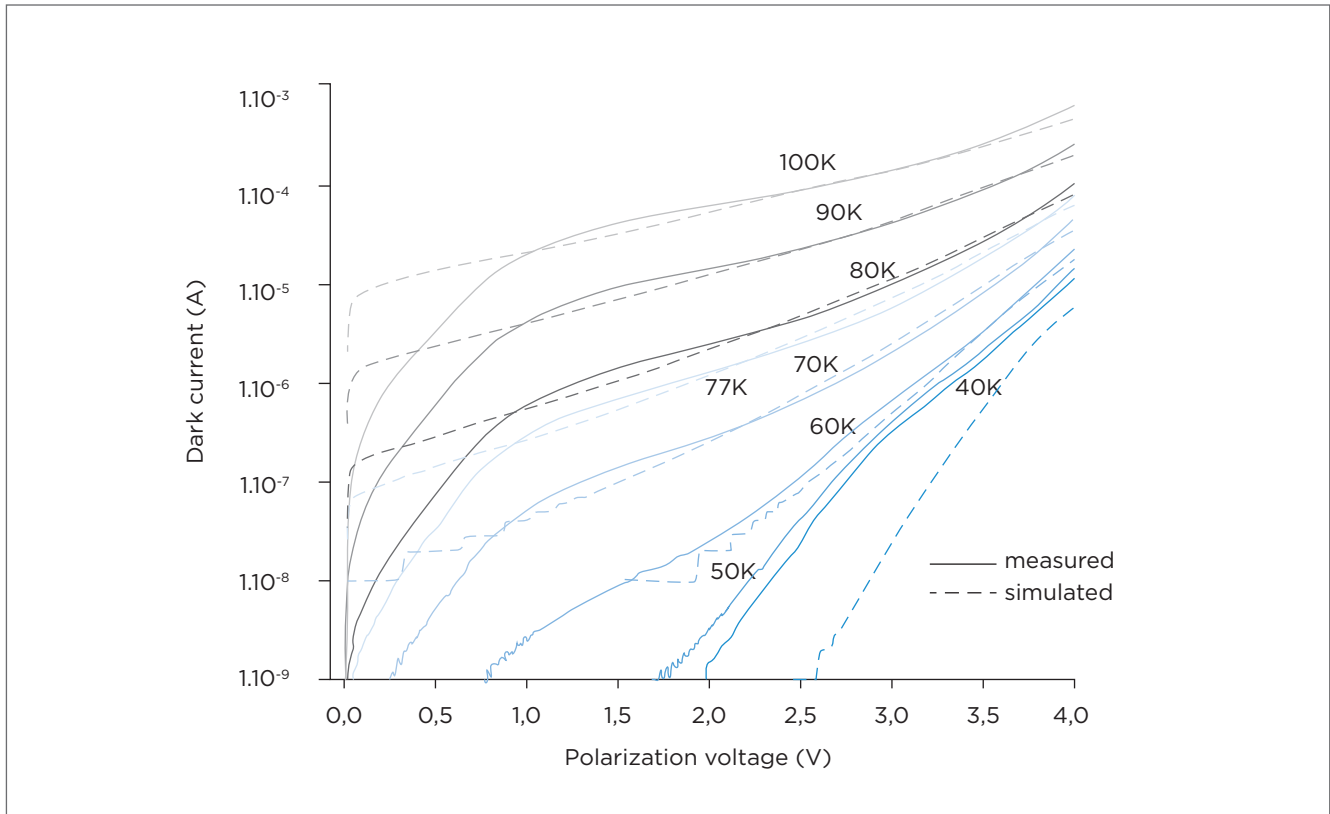


**Figure 11.** Comparison between the curves  $I \times V$  in the dark for sample A in Table 2, for temperatures of 40-100 K (ISSMAEL JUNIOR, 2007).

Simulations were carried out for the normalized responsivity of the photodetector by Alves (2005) – sample A in Table 1 – for voltages of 0.5, 1.0, and 1.5 V, temperature of 10 K. These curves were compared to the measurements taken by Hanson (2006). The error between the simulated and the measured wavelength at the peak was 2.53%, for the polarization voltage of 0.5 V – Figure 12; 1.68% for the polarization voltage of 1.0 V – Figure 13; and 1.17% for the polarization voltage of 1.5 V – Figure 14.

There is consistency between theoretical values and the measurements, with errors lower than 3%, decreasing while the polarization voltage increases. However, it is necessary to improve the model of the absorption coefficient, so that the simulations of responsivity get closer to reality, without using normalization.

#### 4. DISCUSSION AND FINAL OBSERVATIONS

With the objective of investigating the capacity of models in the literature to represent the main figures of

merit of QWIP, many comparisons were made. The difficulty to shape the phenomena at temperatures below 50 K was observed, besides the fact that, due to the high number of factors influencing the figures of merit – such as precision in growth, precision in bandoffset values, effective mass, bandgap, dopant ionization, among others – the absolute values of the amplitude have little significance in theoretical calculations. On the other hand, the methodology used to calculate the confined energy levels and their respective wave functions proved to be efficient (ALVES, 2005). Attempts to adapt the models have been made and require other cycles of manufacture in order to test its effectiveness. These results will be published in other studies.

Finally, the considerations made during the development of this paper cooperate with the effort of the Air Force to improve its technical knowledge in the field of infrared photodetection, aiming at leading our country toward independence and autochthonous development of this strategic field of knowledge.

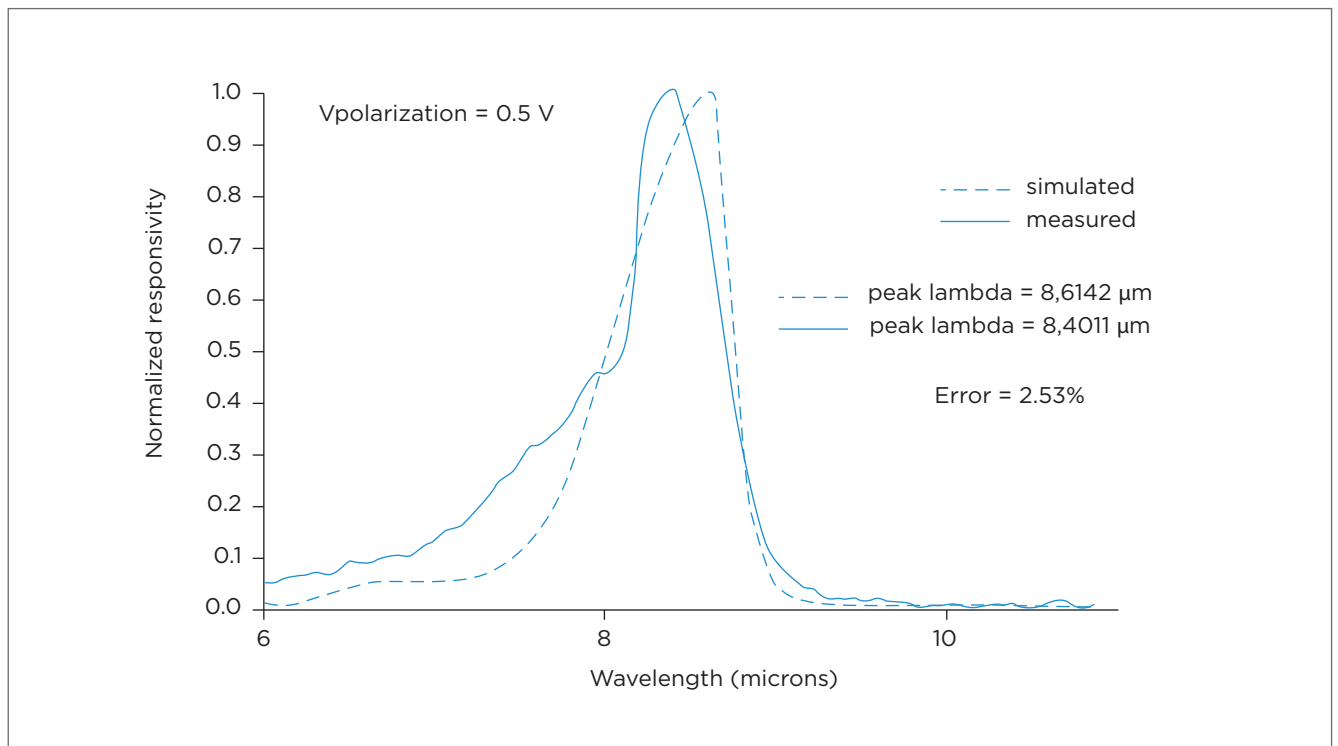


**Figure 12.** Normalized results of simulated and measured responsivity in function of the wavelength for polarization voltage of 0.5 V (ISSMAEL JUNIOR, 2007).

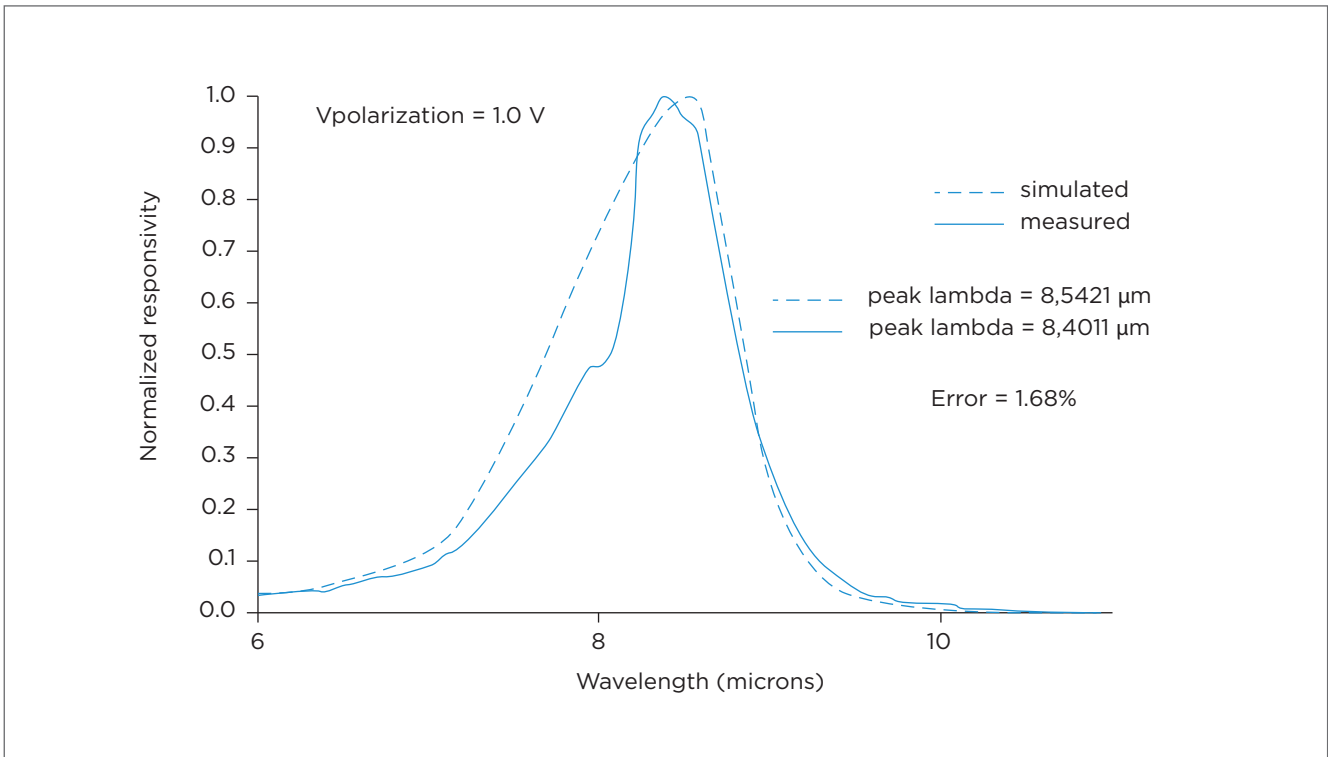


**Figure 13.** Normalized results of simulated and measured responsivity in function of the wavelength for polarization voltage of 1.0 V (ISSMAEL JUNIOR, 2007).

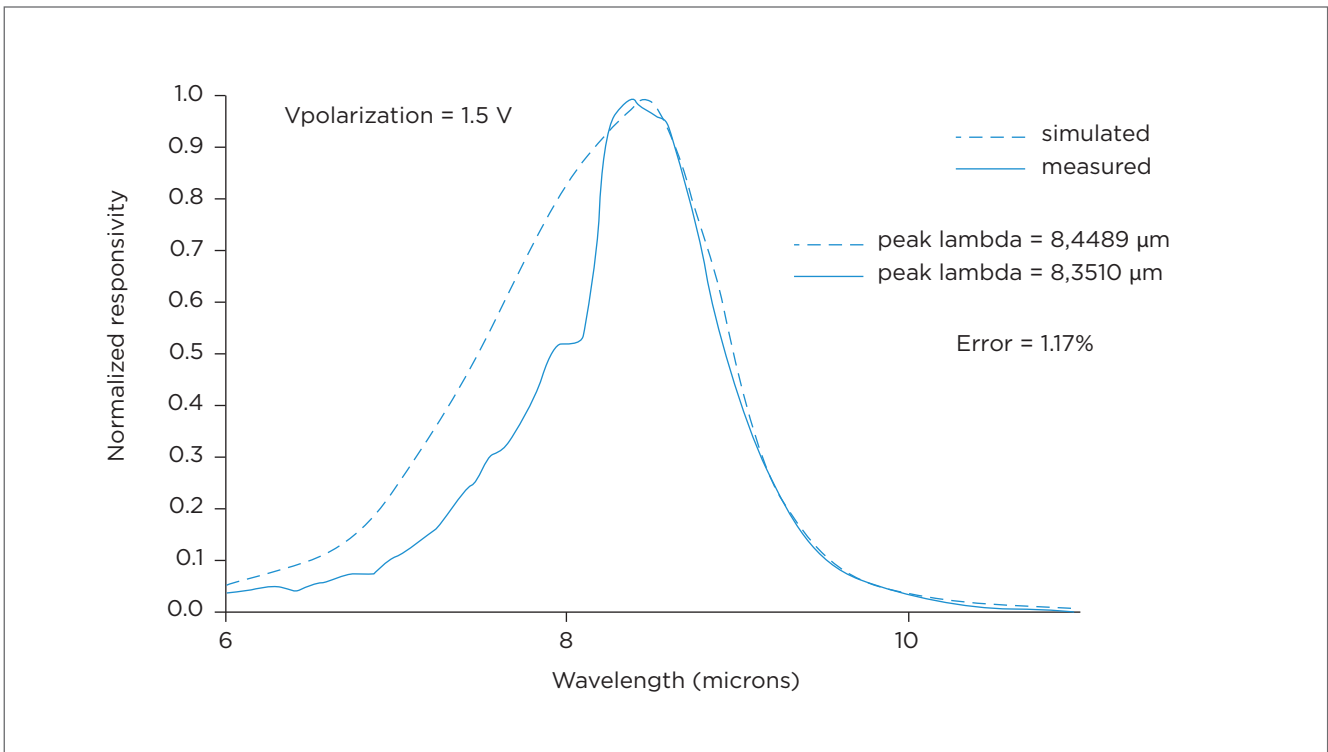


**Figure 14.** Normalized results of simulated and measured responsivity in function of the wavelength for polarization voltage of 1.5 V (ISSMAEL JUNIOR, 2007).

## REFERENCES

- ALVES, F.D.P. *Design and Analysis of a Multicolor Quantum Well Infrared Photodetector*. United States Naval Postgraduate School Master's Thesis, september 2005.
- ALVES, F.D.P.; TAVARES SANTOS, R.A.; AMORIM, J.; ISSMAEL JR., A.K.; KARUMASIRI, G. Widely Separate Spectral Sensitivity Quantum Well Infrared Photodetector Using Interband and Intersubband Transitions. *IEEE Sensors Journal*, v. 8, p. 842-848, 2008.
- ALVES, F.D.P.; KURUNASIRI, G.; HANSON, N.; BYLOOS, M.; LIU, H.C.; BEZINGER, A.; et al. NIR, MWIR and LWIR quantum well infrared photodetector using interband and intersubband transitions. *Infrared Physics & Technology*. Elsevier, v. 50, p. 182-186, 2007.
- ANDREWS, S.R.; MILLER, B.A. Experimental and theoretical studies of the performance of quantum well infrared detectors. *Journal of Applied Physics*, v. 2, n. 70, 1991.
- BOSCHETTI, C. *O espectro infravermelho*. Disponível em: <<http://www.las.inpe.br/-cesar/Infrared/espectro.htm>>. Acesso em: 15 abr. 2015.
- Dyer, W.R; Tidrow, M.Z. QWIP technology applications to ballistic missile defense. *Proceedings of SPIE*, v. 3553, p. 231-238, 1998.
- FU, Y.; WILLANDER, M. Optical coupling in quantum well infrared photodetector by diffraction grating. *Journal of Applied Physics*, v. 84, n. 10, 1998.
- GUNAPALA, S.D. *What is QWIP Technology?*
- GUNAPALA, S.D.; BANDARA, S.V. Quantum Well Infrared Photodetector (QWIP) Focal Plane Arrays. *Semiconductors and Semimetals*, v. 62, 1999.
- GUNAPALA, S.D.; BANDARA, S.V.; LIU, J.K.; SIR RAFOL; SHOTT, C.A.; JONES, R.; et al. 640x512 pixel four-band, broad-band, and narrow-band quantum well infrared photodetector focal plane arrays. Disponível em: <[https://www.researchgate.net/publication/233980001\\_640x512\\_pixel\\_four-band\\_broad-band\\_and\\_narrow-band\\_quantum\\_well\\_infrared\\_photodetector\\_focal\\_plane\\_arrays](https://www.researchgate.net/publication/233980001_640x512_pixel_four-band_broad-band_and_narrow-band_quantum_well_infrared_photodetector_focal_plane_arrays)>. Acesso em: 09 mar. 2007.
- HANSON, N.A. *Characterization and analysis of a multicolor quantum well infrared photodetector*. United States Naval Postgraduate School Master's Thesis, Monterey, California, June 2006.
- HARRISON, P. *Quantum wells, wires and dots: theoretical and computational physics*. 2 ed. Wiley, Chichester, UK, 2005.
- INOVAÇÃO TECNOLÓGICA. Sensor de infravermelho agora é capaz de ver em cores. *Site Inovação tecnológica*, 2006. Disponível em: <<http://inovacaotecnologica.com.br/noticias/noticia.php?artigo=010110060526>>. Acesso em: 15 abr. 2015.
- Institute of Microelectronic's site. *Low Field Mobility*. Disponível em: <<http://www.iue.tuwien.ac.at/phd/quay/node34.html>>. Acesso em: 30 nov. 2014.
- Institute of Microelectronic's site. *Semiconductor Alloys*. Disponível em: <<http://www.iue.tuwien.ac.at/phd/quay/node35.html>>. Acesso em: 30 nov. 2014.
- Institute of Microelectronic's site. *Velocity Saturation*. Disponível em: <<http://www.iue.tuwien.ac.at/phd/palankovski/node48.html>>. Acesso em: 30 nov. 2014.
- Issmael Junior, A.K. *Estudo, modelamento e simulação das principais figuras de mérito de fotodetectores infravermelhos à poços quânticos*. 106 f. Monografia – Instituto Tecnológico de Aeronáutica, São José dos Campos, 2007.
- ISSMAEL JR, A.K.; ALVES, F.D.P.; TAVARES SANTOS, R.A. *Estudo, modelamento e simulação das principais figuras de mérito de fotodetectores infravermelhos à poços quânticos*. IX Simpósio de Guerra Eletrônica, 2007. Disponível em: <[http://www.sige.ita.br/anais/IXSIGE/Artigos/GE\\_01.pdf](http://www.sige.ita.br/anais/IXSIGE/Artigos/GE_01.pdf)>. Acesso em: 15 abr. 2015.
- Levine, B.F. Quantum well infrared photodetectors. *Journal of Applied Physics*, v. 8, n. 74, 1993.
- MISSILE DEFENSE AGENCE. *Site da MDA*.
- NATIONAL AERONAUTICS AND SPACE ADMINISTRATION (NASA). *My NASA Data site*. Disponível em: <<http://mynasadata.larc.nasa.gov/ElectroMag.html>>. Acesso em: 24 mar. 2007.
- SANTOS, R.A.T. *Proposta de Metodologia para Estimação do Envelope Infravermelho de Aeronaves*. Tese (Mestrado) – Instituto Tecnológico de Aeronáutica, São José dos Campos, 2004.
- VURGAFTMAN, I.; MEYER, J.R.; RAM-MOHAN, L.R. Band parameters for III-V compound semiconductors and their alloys. *Journal of Applied Physics Review*, v. 89, n. 11, p. 5815-5875, 2001.